AMERICAN SOCIETY FOR MICROBIOLOGY | Journal of Bacteriology®

MEETING PRESENTATION

Alternative Oxidase Activity Reduces Stress in *Vibrio fischeri* Cells Exposed to Nitric Oxide

Anne K. Dunn[a]

[a]Department of Microbiology and Plant Biology, University of Oklahoma, Norman, Oklahoma, USA

ABSTRACT Alternative oxidase (Aox) is a non-energy-conserving respiratory oxidase found in certain eukaryotes and bacteria, whose role in physiology is not entirely clear. Using the genetically tractable bacterium *Vibrio fischeri* as a model organism, I have identified a role for Aox to reduce levels of stress in cells exposed to oxygen and nitric oxide (NO). In *V. fischeri* lacking the NO-detoxifying enzyme flavohemoglobin (Hmp), deletion of *aox* in cells grown in the presence of oxygen and NO results in alterations to the transcriptome that include increases in transcripts mapping to stress-related genes. Using fluorescence-based reporters, I identified corresponding increases in intracellular reactive oxygen species and decreases in membrane integrity in cells lacking *aox*. Under these growth conditions, activity of Aox is linked to a decrease in NADH levels, indicating coupling of Aox activity with NADH dehydrogenase activity. Taken together, these results suggest that Aox functions to indirectly limit production of ferrous iron and damaging hydroxyl radicals, effectively reducing cellular stress during NO exposure.

IMPORTANCE Unlike typical respiratory oxidases, alternative oxidase (Aox) does not directly contribute to energy conservation, and its activity would presumably reduce the efficiency of respiration and associated ATP production. Aox has been identified in certain bacteria, a majority of which are marine associated. The presence of Aox in these bacteria poses the interesting question of how Aox function benefits bacterial growth and survival in the ocean. Using the genetically tractable marine bacterium *Vibrio fischeri*, I have identified a role for Aox in reduction of stress under conditions where electron flux through the aerobic respiratory pathway is inhibited. These results suggest that Aox activity could positively impact longer-term bacterial fitness and survival under stressful environmental conditions.

KEYWORDS *Aliivibrio fischeri*, RNA-seq, Fenton chemistry, *Vibrio fischeri*, nitric oxide, oxidase, respiration

Alternative oxidase (AOX [eukaryotes] or Aox [bacteria]) is a terminal respiratory oxidase present in all plants as well as certain other eukaryotes (1). The activity of this protein does not directly contribute to the generation of a proton motive force (2), a characteristic that is atypical of respiratory oxidases. AOX has been well studied in plants, where its non-energy-conserving activity is known to reduce the energy efficiency of plant respiration. Although seemingly wasteful, AOX has been linked to useful activities such as heat production in thermogenic plants (3). The role of this protein in nonthermogenic plants is not as clear, but it is believed to play a role in modulating metabolic state and/or signaling during stress (4), as well as affecting energy and carbon metabolism in plants under nonstress conditions (5). Understanding the specific roles of AOX in nonthermogenic plants and other eukaryotic organisms is currently an active area of research.

The discovery of Aox in bacteria is relatively more recent, coinciding with the availability of increased amounts of genomic and environmental metagenomic se-

Received 31 December 2017 **Accepted** 7 May 2018

Accepted manuscript posted online 14 May 2018

Citation Dunn AK. 2018. Alternative oxidase activity reduces stress in *Vibrio fischeri* cells exposed to nitric oxide. J Bacteriol 200:e00797-17. https://doi.org/10.1128/JB.00797-17.

Editor Victor J. DiRita, Michigan State University

Address correspondence to akdunn@ou.edu.

quencing data (6–8). The number of bacteria predicted to encode Aox continues to grow as more genomes and environmental samples are sequenced, and based on database searches, a majority of *aox*-like genes are found in marine environment-associated bacterial isolates and marine metagenome samples. Examples include an abundance of *aox*-like sequences in the metagenomic data sets from the Global Ocean Sampling expedition (9) and the Sargasso Sea (7) and the presence of *aox* in a cultivated member of the SAR11 group of numerically dominant marine bacteria (*Pelagibacter* spp.) (10). In addition, based on genome sequence data, it appears that *aox*-like genes are fairly widespread, although not ubiquitous, in *Vibrio* spp. (reference 11 and data not shown). The presence of *aox*-like genes in these data sets suggests an importance of Aox function for the growth and survival of certain bacteria in the ocean. However, the role of Aox in bacterial physiology is not yet clear, as detailed studies have been limited by availability of isolates and/or genetically manipulable isolates. We previously discovered an Aox-encoding gene in the marine bacterium *Vibrio fischeri* (*Aliivibrio fischeri*) strain ES114 (12) and are using this genetically tractable bacterium to better understand the physiological benefit of Aox function in bacteria.

V. fischeri ES114 was isolated from the Hawaiian bobtail squid, *Euprymna scolopes* (13), and is used as a model strain in studying this mutualistic light organ symbiosis (14). Aox is expressed in *V. fischeri* ES114 in response to nitric oxide (NO) and, unlike the other terminal oxidases in this bacterium, is resistant to inhibition by NO (12). It is known that *V. fischeri* encounters host-produced NO during symbiotic colonization (15), and therefore, the response to NO is physiologically relevant in the natural environments this bacterium inhabits.

Based on these previous results, I hypothesized that the physiological benefit of Aox function is relevant to conditions where both oxygen and NO are present and there is flux through the aerobic respiratory pathways. Under these conditions, NO would be expected to inhibit the NO-sensitive respiratory oxidases while inducing expression of the NO-resistant Aox. Aox could then function to allow electron flow, which could positively impact the cell in various ways. Here, I demonstrate that in a strain lacking the main aerobic NO-detoxifying protein Hmp (16), Aox contributes to reducing NADH levels while also decreasing the levels of reactive oxygen species and membrane damage in cells exposed to NO. These results indicate that a physiological benefit of Aox function in *V. fischeri* is to reduce cellular stress during NO exposure, which could positively impact longer-term fitness and survival.

RESULTS

A lack of *aox* in a *V. fischeri hmp* mutant background affects growth in the presence of nitric oxide. Although a strain lacking *aox* did not display phenotypic differences from the wild type under previously tested growth conditions (12), deletion of this gene in a *V. fischeri* strain lacking the aerobic NO-detoxifying enzyme flavohemoglobin (Hmp) (16) resulted in an alteration in the growth phenotype of cells grown in glucose mineral salts medium containing the NO-generating compound dipropylenetriamine (DPTA)-NONOate (Fig. 1). This growth phenotype could be complemented by providing *aox* in *trans* under the control of an inducible promoter. A similar growth phenotype was observed in mineral salts medium containing NO and either *N*-acetylglucosamine or glycerol as the carbon source (data not shown).

***V. fischeri* cells lacking *aox* and *hmp* have higher plating efficiency on solid medium after NO treatment.** To determine whether the growth phenotype observed during NO treatment was due to differences in the number of cells present in the cultures, AKD915 (Δ*hmp*) and AKD916 (Δ*hmp* Δ*aox*) were grown in mineral salts medium and samples removed 6 h after NO treatment for direct counting and plating to determine recoverable CFU (Fig. 2B). No significant difference between the numbers of cells of the two strains were observed by direct counting ($P > 0.05$). However, a significantly higher number of CFU were observed from the cultures lacking *aox*, suggesting that these cells were better able to cope with the transition from mineral salts liquid medium to rich solid medium. No significant differences in direct counts or

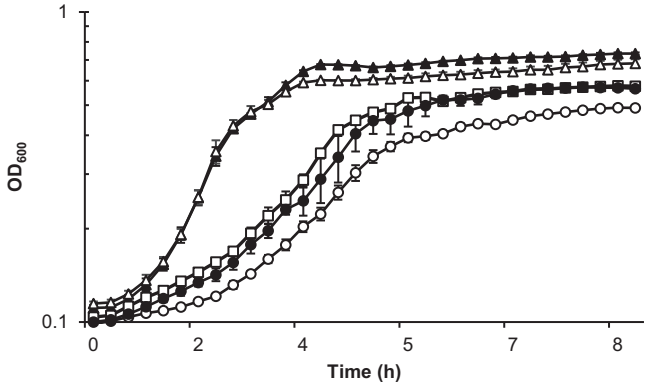

FIG 1 A *V. fischeri* strain lacking *hmp* and *aox* displays an altered growth phenotype in mineral salts medium with nitric oxide. *V. fischeri* strains ES114 (wild type; white triangles), AKD915 (Δ*hmp*; white squares), AKD916 (Δ*hmp* Δ*aox*; white circles), and AKD916 containing the *aox*-complementing plasmid pAKD601Baox (black circles) were grown in mineral salts medium and treated with DPTA-NONOate. Data are also shown for the wild-type strain grown in the absence of DPTA-NONOate (black triangles). There was no difference in growth between the wild type, AKD915, and AKD916 when grown in the absence of DPTA-NONOate (data not shown). Experiments were repeated three times, and the results of one representative experiment are shown.

plating efficiency were observed between the wild-type strain (ES114) and AKD915 and AKD916 in the absence of NO treatment (Fig. 2A), indicating that this plating efficiency phenotype was linked to NO treatment. Previous work in *Escherichia coli* identified that when cells were transferred from liquid to solid medium, global stress responses were induced (17). If *V. fischeri* cells lacking *aox* experienced higher levels of stress when treated with NO in liquid medium, then it is plausible that these stress response pathways would be upregulated and help the cells transition from liquid to solid medium.

Transcriptome analysis identifies alterations in gene expression in AKD916 (Δ*hmp* Δ*aox*), including genes likely involved in stress responses. To determine whether there were significant alterations in the transcriptomes of AKD915 (Δ*hmp*) and AKD916 (Δ*hmp* Δ*aox*) grown in the presence of nitric oxide, cells were grown in glucose mineral salts medium with DTPA-NONOate for 6 h prior to harvesting total RNA for transcriptome sequencing (RNA-seq) analysis. Analysis of these data using Rockhopper (18) identified 602 differentially regulated transcripts (410 upregulated and 192 downregulated) (see Data Set S1 in the supplemental material). Of the nine sense transcripts identified as having a 4.5-fold or greater induction in AKD916 compared to AKD915, two mapped to open reading frames (ORFs) annotated as encoding hypothetical proteins (VF_A0006 and VF_A0314), and five mapped to ORFs annotated as encoding stress-related proteins (VF_1685, VF_A0005, VF_A0311, VF_A0312, and VF_A0313) (Table 1). RNA-seq results were verified for a subset of Rockhopper-predicted upregulated and downregulated genes using quantitative reverse transcriptase PCR (qRT-PCR) (Fig. 3).

Aox function under NO treatment reduces intracellular reactive species levels and improves membrane integrity. Transcriptome analysis suggested that *V. fischeri* cells lacking a functional Aox were experiencing more cellular stress when treated with NO. To attempt to measure increased levels of stress, cells grown in mineral salts medium were harvested 6 h after NO treatment and stained with fluorescent indicators for reactive oxygen species (aminophenyl fluorescein [APF]) or membrane integrity (SYTO 9 and propidium iodide [LIVE/DEAD BacLight assay]). Compared to AKD915 (Δ*hmp*) cells, AKD916 (Δ*hmp* Δ*aox*) cells had significantly higher levels of fluorescence when treated with APF and higher levels of red fluorescence when treated with SYTO 9 and propidium iodide, indicating higher levels of hypochlorite, peroxynitrite, and/or the hydroxyl radical and increased membrane damage, respectively (Table 2). These results support the hypothesis that cells lacking Aox experience higher levels of cellular stress when treated with NO.

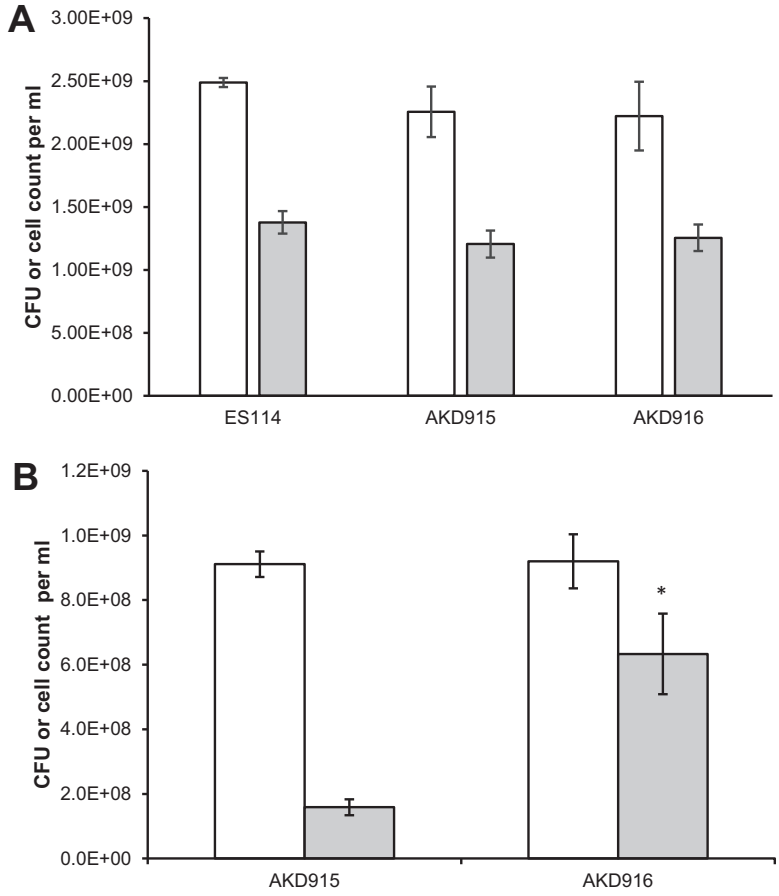

FIG 2 Cell recovery via direct count versus plating of the wild-type strain (ES114), AKD915 (Δ*hmp*), and AKD916 (Δ*hmp* Δ*aox*) after growth in mineral salts medium either without (A) or with (B) nitric oxide treatment. Cells were grown in mineral salts medium and, where indicated, treated with DPTA-NONOate. After 6 h, samples were removed for direct counts using a Petroff-Hausser counter (white bars) and plating onto rich medium (gray bars) to determine recoverable CFU. (A) In the absence of nitric oxide, there was no significant difference ($P > 0.05$) between strains in direct cell counts or CFU recovered after plating. (B) After treatment with nitric oxide, more CFU of a *V. fischeri* strain lacking *hmp* and *aox* (AKD916) than of the parental strain lacking *hmp* (AKD915) were recovered. Significance for comparisons between direct counts of AKD915 and AKD916 or between plating recovery for AKD915 and AKD916 was measured using Student's *t* test. *, $P < 0.04$. No significant difference was detected between direct counts or plating recovery for wild-type cells grown in the presence or absence of NO ($P > 0.05$) (data not shown). Data shown are averages (±standard error) from one representative experiment containing three independent cultures. Experiments were repeated three times.

***V. fischeri* AKD916 (Δ*hmp* Δ*aox*) has higher levels of NADH when grown in the presence of NO.** Previously, we showed that *V. fischeri* Aox is induced in response to nitric oxide and functions as a NO-resistant oxidase terminating the electron transport chain (12). If activity of Aox was coupled to the activity of a NADH dehydrogenase in

TABLE 1 Sense transcripts with 4.5-fold or greater induction in *V. fischeri* AKD916 (Δ*hmp* Δ*aox*) compared to AKD915 (Δ*hmp*)

ORF	Annotation	Fold induction
VF_1685	*recR*; recombination protein RecR	5.2
VF_1735	*acpP*; acyl carrier protein	4.9
VF_A0005	*msrAB*; peptide-methionine (*S*)-*S*-oxide reductase	5.7
VF_A0006	Hypothetical protein	5.8
VF_A0311	*pspA*; regulatory protein for phage shock protein operon	4.5
VF_A0312	*pspB*; phage shock protein B	5.6
VF_A0313	*pspC*; phage shock protein C	5.5
VF_A0314	*ycjX*; hypothetical protein	5.1
VF_A0364	Transporter	5.1

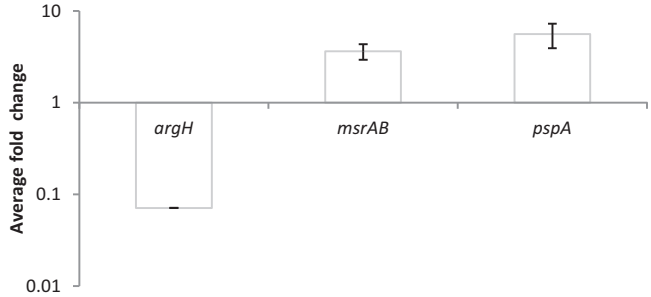

FIG 3 Quantitative real-time PCR results for selected genes identified as differentially expressed in the Rockhopper analysis of RNA-seq data. The results demonstrate relative transcript levels of *argH* (VF_2303), *msrAB* (VF_A0005), and *pspA* (VF_A0311) in AKD916 (Δ*hmp* Δ*aox*) compared to AKD915 (Δ*hmp*) after 6 h of growth in mineral salts medium containing the nitric oxide generator DPTA-NONOate. Relative gene expression was measured using the relative standard curve method and *ftsK* (VF_0905) as an endogenous control. The trend in gene expression levels agrees with the Rockhopper analysis (Table 1; see Data Set S1 in the supplemental material). Data are the averages from three separate PCR runs, one for each of three independent replicates.

the electron transport chain, a lack of Aox under these conditions should result in higher cellular NADH levels. To test this, samples of AKD915 (Δ*hmp*) and AKD916 (Δ*hmp* Δ*aox*) were harvested after 6 h of growth in mineral salts medium containing DPTA-NONOate, and the levels of NAD^+ and NADH were assayed. After 6 h of growth, AKD916 had significantly higher levels of NADH than AKD915, indicating that under these conditions, Aox activity is coupled to the activity of an NADH dehydrogenase (Fig. 4). It has been previously shown that increased levels of NADH can promote oxidative DNA damage in *E. coli* (19), suggesting a possible link between Aox function, NADH levels, and cellular stress in *V. fischeri*.

Addition of the iron chelator 2,2′-bipyridyl or the antioxidant glutathione to cultures can partially reverse the NO-induced *aox* mutant growth phenotype. Oxidative DNA damage in *E. coli* in response to increased levels of NADH is mediated through Fenton chemistry (19), where NADH indirectly contributes to the reduction of iron to the ferrous state. The ferrous iron then participates in the Fenton reaction to generate the DNA-damaging hydroxyl radical. If a similar situation was occurring in *V. fischeri* cells lacking Aox, then addition of the ferrous iron chelator 2,2′-bipyridyl or the antioxidant glutathione to NO-treated cultures should result in less stress and a less pronounced growth phenotype. Addition of either of these compounds did reduce the magnitude of the growth phenotype of cells lacking Aox (Fig. 5), indicating that under these conditions, Aox functions to reduce NADH levels and therefore presumably indirectly reduces production of ferrous iron and damaging hydroxyl radicals.

TABLE 2 Fluorescence-based assays for reactive oxygen species production and membrane integrity in *V. fischeri* strains treated with nitric oxide

	Reactive oxygen species (APF)		Membrane integrity (LIVE/DEAD)	
Strain[a]	Avg fluorescence (SE)	*P* value[b]	Avg green/red fluorescence (SE)	*P* value
AKD915 (Δ*hmp*)	635 (32)	0.018	129 (11)	0.026
AKD916 (Δ*hmp* Δ*aox*)	909 (33)		88 (8)	
AKD916 with pAKD601Baox				
Without IPTG	782 (13)	0.0007	91 (3)	0.011
With 0.1 mM IPTG	646 (11)		128 (7)	

[a]Representative data shown for the comparison of AKD915 and AKD916 were collected in an experiment separate from that for the comparison of AKD916(pAKD601Baox) with and without IPTG.
[b]*P* value calculated using Student's *t* test comparing AKD915 with AKD916 or comparing AKD916(pAKD601Baox) with and without IPTG.

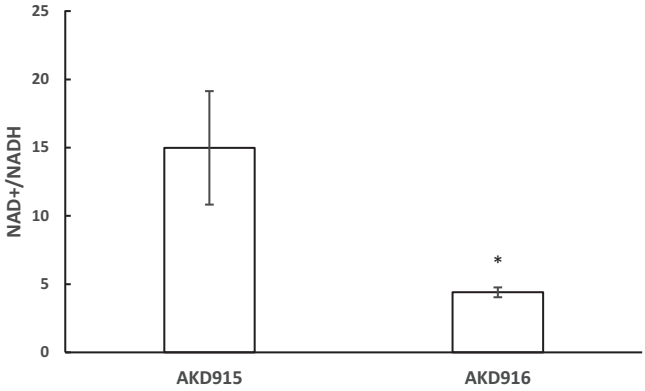

FIG 4 A *V. fischeri* strain lacking *hmp* and *aox* has elevated NADH levels 6 h after treatment with nitric oxide. *V. fischeri* strains AKD915 (Δ*hmp*) and AKD916 (Δ*hmp* Δ*aox*) were grown in mineral salts medium and treated with DPTA-NONOate. Samples were taken 6 h after treatment and assayed for NAD^+ and NADH levels. AKD915 samples had an average of 1.25 (±0.098) μM NAD^+ plus NADH and AKD916 samples had an average of 1.68 (±0.16) μM NAD^+ plus NADH. Data shown are the averages from three experiments, each containing three independent replicates. Significance was measured using Student's *t* test. *, $P < 0.02$.

DISCUSSION

The results of this study identify a function for bacterial alternative oxidase in reduction of cellular stress under conditions where electron flux through the aerobic respiratory pathway is inhibited. We previously demonstrated that in *V. fischeri* ES114, addition of NO to cultures reversibly inhibits activity of the typical respiratory oxidases while at the same time inducing expression of Aox, an NO-resistant oxidase (12). This induction of Aox activity would allow electron flow through the respiratory pathway in the presence of NO. This would likely be at a lower energy efficiency because Aox activity is not directly linked to the generation of the proton motive force, but it presumably would have other cellular benefits under these growth conditions. To test this hypothesis, I used a *V. fischeri* strain lacking a main aerobic NO-detoxifying enzyme, Hmp, to create a situation where NO was not removed as quickly in cells to allow better observation of the effect of Aox activity on cellular processes. Using this Δ*hmp* strain background, I observed that Aox activity did have significant positive impacts on the cells, resulting in lower levels of NADH, lower levels of reactive oxygen species, and less cellular membrane damage.

V. fischeri ES114 has flexible respiratory pathways (20) and could couple oxidase activity with several different dehydrogenases during respiration. However, under these conditions, my results suggest that Aox activity is coupled to the activity of an NADH dehydrogenase, as lack of Aox results in higher levels of cellular NADH (Fig. 3). Excess NADH could contribute to increased cellular stress similarly to the case in *E. coli*, where higher NADH levels promoted oxidative DNA damage (19). In *E. coli*, it was demonstrated that NADH indirectly contributes to the reduction of iron to the ferrous state, which then can participate in a Fenton chemistry reaction to produce DNA-damaging hydroxyl radicals (19). Several lines of experimental evidence support this scenario in *V. fischeri*. Transcriptome analysis identified increased levels of transcripts mapping to genes whose products could be involved in stress responses, including DNA damage repair (*recR*) (Table 1; see Data Set S1 in the supplemental material) and membrane stress (*pspA*, *pspB*, and *pspC*) (Table 1 and Data Set S1) (21). In addition, cells lacking Aox had a significantly higher level of fluorescence when treated with the reactive oxygen species indicator APF, which detects hypochlorite, peroxynitrite, and the hydroxyl radical (Table 2). Finally, addition of the ferrous iron chelator 2,2′-bipyridyl or the antioxidant glutathione reduced the severity of the growth phenotype in the strain lacking Aox (Fig. 5). Taken together, these data support the function of Aox to allow electron flow under conditions where the aerobic electron transport chain activity is

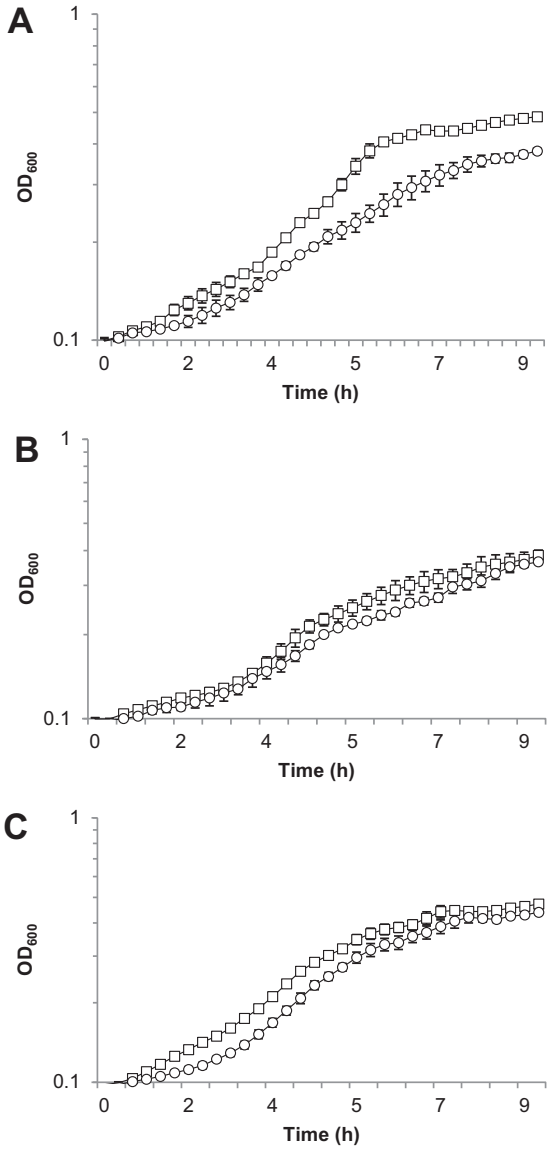

FIG 5 The nitric oxide-induced growth phenotype of the *V. fischeri* strain lacking *hmp* and *aox* can be partially complemented by providing the iron chelator 2,2′-bipyridyl or the antioxidant glutathione. AKD915 (Δ*hmp*; squares) and AKD916 (Δ*hmp* Δ*aox*; circles) were grown in mineral salts medium containing DPTA-NONOate alone (A) or with the addition of 50 μM 2,2′-bipyridyl (B) or 1 mM glutathione (C). Experiments were repeated three times, and the results of one representative experiment are shown.

inhibited, effectively reducing intracellular stress. Further studies will explore how Aox activity contributes to longer-term fitness and survival.

It remains to be determined whether Aox regulation and function are similar in other marine bacteria. Our unpublished preliminary data using quantitative RT-PCR suggest that NO does induce *aox* transcript levels in other marine bacteria, including alphaproteobacterial and gammaproteobacterial isolates. In the case of *V. fischeri*, it is known that NO is encountered during host colonization (15), which might not be relevant to the lifestyle(s) of other marine bacteria. However, it is known that denitrifying bacteria can produce NO that affects surrounding microbes (22), which could be relevant in certain marine environments inhabited by bacteria encoding Aox. Even if NO does not universally induce Aox expression in all Aox-containing bacteria, it is possible that other conditions that impact normal electron flow through the respiratory pathway induce Aox expression, resulting in

TABLE 3 Strains and plasmids

Strain or plasmid	Description[a]	Reference or source
Strains		
Vibrio fischeri		
ES114	Wild type	13
AKD915	Δ*hmp* (allele exchanged from pAKD915 into ES114)	This study
AKD916	Δ*hmp* Δ*aox* (allele exchanged from pAKD780 into AKD915)	This study
Escherichia coli		
DH5α	F$^-$ ϕ80d*lacZ*ΔM15 Δ(*lacZYA-argF*)*U169 deoR supE44 hsdR17 recA1 endA1 gyrA96 thi-1 relA*	31
DH5αλ*pir*	λ*pir* derivative of DH5α	32
CC118λ*pir*	Δ(*ara-leu*) *araD* Δ*lacX74 galE galK phoA20 thi-1 rpsE rpoB argE*(Am) *recA*; lysogenized with λ*pir*	27
Plasmids		
pAKD915	Δ*hmp* allele, R6Kγ and ColE1 replication origins, RP4 *oriT*, Erm^r Kan^r	This study
pAKD780	Δ*aox* allele, R6Kγ and ColE1 replication origins, RP4 *oriT*, Erm^r Kan^r	12
pAKD601Baox	Plasmid containing *lacI*^{q} and an IPTG-inducible promoter for controlled expression of Aox in *V. fischeri*, Kan^r	12
pEVS104	Conjugative helper plasmid, R6Kγ replication origin, Kan^r	27

[a]Erm^r, erythromycin resistance; Kan^r, kanamycin resistance (*aph*).

a similar protective mechanism against cellular stress. The results reported here lay the foundation for further exploration of the conservation of Aox function in diverse bacteria and how activity of this interesting protein impacts bacterial growth and survival in marine environments.

More broadly, understanding the role of Aox in bacteria will allow functional comparisons to eukaryotic AOX and investigations into the evolutionary history of this protein. In certain plants, AOX activity is induced in response to stress and may contribute to reduction in the production of reactive oxygen species (23), suggesting that there may be similarities in Aox function in bacteria and eukaryotes. Studying AOX in plants has been complicated by the presence of multiple genes encoding different versions of the protein which can be used under different situations with different outcomes (24), making studies involving the physiological role of AOX difficult. Bacteria typically contain a single copy of an *aox*-like gene, with certain isolates being more amenable to genetic manipulation, which can simplify functional studies. In addition, it has been postulated that AOX was acquired from bacteria by eukaryotes during endosymbiosis events that created mitochondria (7). Therefore, studying Aox function and distribution in bacteria also has implications for understanding the evolutionary history of this protein.

MATERIALS AND METHODS

Strains, plasmids, and growth conditions. The strains and plasmids used in this study are listed in Table 3. *Escherichia coli* was grown in LB medium (25) with 40 μg/ml kanamycin where noted or in HiVeg Special Infusion broth (Himedia, Mumbai, India) containing 150 μg/ml erythromycin. *Vibrio fischeri* was grown either in LB medium with added salt (LBS) (26) or in mineral salts medium with 20 mM glucose as the carbon source, containing the following (per liter): 378 ml 1 M $NaPO_4$ (pH 7.5), 50 ml 1 M Tris (pH 7.5), 3 mg $FeSO_4 \cdot 7H_2O$, 0.59 g NH_4Cl, 13.6 g $MgSO_4 \cdot 7H_2O$, 0.83 g KCl, 1.62 g $CaCl_2$, 1 g Casamino Acids (Difco, vitamin assay), and, where noted, 100 μg/ml kanamycin. Where indicated, dipropylenetriamine (DPTA)-NONOate (Cayman Chemical, Ann Arbor, MI) was added to cultures to a final concentration of 200 μM. DPTA-NONOate is a nitric oxide (NO) donor with a half-life of 5 h at 22 to 25°C and pH 7.4 to liberate 2 mol of NO per mol of parent compound. For complementation assays, 0.1 mM isopropyl-β-D-thiogalactopyranoside (IPTG) (Research Products International), 50 μM 2,2′-bipyridyl (Sigma, St. Louis, MO), or 1 mM glutathione (Sigma) was added to cultures where indicated.

General cloning procedures were used with *E. coli*, and constructs containing the RP4 origin of transfer were introduced into *V. fischeri* using triparental mating (27). *E. coli* DH5α λ*pir* was used for plasmid construction, and *E. coli* DH5α, DH5α λ*pir*, or CC118 λ*pir* was used for conjugative transfer of plasmids into *V. fischeri*. Plasmids were constructed using standard molecular biology techniques and restriction enzymes from New England BioLabs (Ipswich, MA). PCR products were amplified using Phusion high-fidelity DNA polymerase (New England BioLabs) with primers from Integrated DNA Technologies (Coralville, IA). Primer sequences are listed in Table 4.

V. fischeri strains lacking *hmp* (VF_2316) or *aox* (VF_0578) were constructed using allelic exchange (28). Briefly, approximately 1.6 kb of DNA upstream of each target was PCR amplified and fused to an approximately 1.6-kb DNA fragment downstream of each gene using an engineered restriction site. The PCR products included the respective start and stop codons and additional flanking codons as needed for primer design.

TABLE 4 Primers used in this study

Primer name	Primer sequence (5′→3′)	Use
hmpupF	GAGTTACCACGCTGAATCGCT	Forward primer for upstream fragment for *hmp* deletion construct
hmpupR	TTATAAAAATTAGTCGACGTTGAGCATATTGTTTACCTTTAAAGGTGTA	Reverse primer for upstream fragment for *hmp* deletion construct
hmpdownF	CAATATGCTCAACGTCGACTAATTTTTATAAAGTAGAAATGCAAAAACGCCCA	Forward primer for downstream fragment for *hmp* deletion construct
hmpdownR	CACGGTACTTACCCTTACGTAACATC	Reverse primer for downstream fragment for *hmp* deletion construct
hmpRepF	TACTACCTAGGACGCTTGCTTTGCTTTCGCT	Used with hmpTestR to screen for *hmp* deletion mutants
hmpTestR	TCTGTTACTGCTGATGGACGTAAACAT	
msrAB F	CGCAAGAAGAGGGAACAGAA	Forward primer for qRT-PCR of VF_A0005
msrAB R	CCAACCAGTCCCGGATTTATAC	Reverse primer for qRT-PCR of VF_A0005
pspA F	CCAACAAACTGCACAGCATAG	Forward primer for qRT-PCR of VF_A0311
pspA R	CTCATCAATTCGGCGTTCATATT	Reverse primer for qRT-PCR of VF_A0311
argH F	ATTGGCTGATACCGTGACTTC	Forward primer for qRT-PCR of VF_2303
argH R	CCATATACACGTCCACACTTACC	Reverse primer for qRT-PCR of VF_2303
ftsZ F	GTGCGTGTCGTTGAAGTTATTC	Forward primer for qRT-PCR of VF_0905
ftsZ R	GGCTACCTACAACATCAGAGAAG	Reverse primer for qRT-PCR of VF_0905

For the *hmp* deletion construct, two codons after the start were included, and for the *aox* deletion construct, two codons prior to the stop were included. These constructs resulted in replacement of the genes with several codons and a 6-bp restriction enzyme recognition site. Primers are listed in Table 4.

Microplate-based growth curves. *V. fischeri* strains were grown overnight in LBS medium, and 12 μl was subcultured into 18-mm culture tubes containing 3 ml of glucose mineral salts medium. Tubes were incubated with vigorous shaking at 28°C. After 1.5 h, 200-μl samples were removed and placed into the wells of a lidded 96-well microtiter dish (Falcon 351172 flat-bottom sterile polystyrene plate). For samples exposed to NO, DPTA-NONOate was added to a final concentration of 200 μM. For complementation assays, IPTG, 2,2′-bipyridyl, or glutathione was added. The plate was incubated at 28°C with double orbital shaking (slow speed, 282 cpm, 3-mm radius) in a BioTek Synergy H1 plate reader (Winooski, VT). Absorbance at 600 nm was measured every ~16 min for ~9 h.

Flask-based growth. For experiments involving direct cell counts and CFU recovery, transcriptome analysis, fluorescence-based assays for reactive oxygen species and membrane integrity, and NAD^+/NADH assays, flask-based cultures were used. Strains were grown overnight in LBS medium, and 60 μl was subcultured into 125-ml flasks containing 15 ml of glucose mineral salts medium. Flasks were incubated with vigorous shaking at 28°C. After 1.5 h, where indicated, DPTA-NONOate was added to each flask to a final concentration of 200 μM. Samples were collected 6 h after addition of DPTA-NONOate. Absorbance at 600 nm was measured using a Bio-Rad SmartSpec Plus spectrophotometer (Hercules, CA).

Direct cell counts and CFU recovery. Cultures were grown as described above for flask-based growth. Three independent replicates of the wild-type strain ES114, AKD915, and AKD916 were grown in mineral salts medium. Samples were collected at 7.5 h for experiments without DPTA-NONOate (Fig. 2A) (ES114 average optical density at 600 nm [OD_{600}], 2.17 ± 0.02; AKD915 average OD_{600}, 2.19 ± 0.01; AKD916 average OD_{600}, 2.09 ± 0.05) or 6 h after addition of DPTA-NONOate (Fig. 2B) (ES114 average OD_{600}, 1.97 ± 0.07; AKD915 average OD_{600}, 0.82 ± 0.01; AKD916 average OD_{600}, 0.73 ± 0.005). Cells were directly counted using a Petroff-Hausser counting chamber (Hausser Scientific Co., Horsham, PA). For each sample, the bacteria within three 50-μm squares were counted and averaged. This number was multiplied by 20,000,000 according to the manufacturer's directions to determine the number of bacteria per milliliter. For CFU recovery, samples were spot dilution plated (29) onto LBS medium and incubated overnight at 28°C prior to counting. Data presented are the average for three independent cultures from one representative experiment, with error bars indicating standard error. Experiments were repeated three times with similar results. Significance was measured using Student's *t* test.

Transcriptome analysis using RNA-seq. Cultures were grown as described above for flask-based growth. Three independent replicates each of AKD915 and AKD916 were grown in mineral salts medium. Samples were collected at 6 h after addition of DPTA-NONOate (AKD915 average OD_{600}, 0.84 ± 0.01; AKD916 average OD_{600}, 0.69 ± 0.003). Two-milliliter culture samples were treated with RNAprotect Bacteria Reagent (Qiagen) following the manufacturer's protocol, and the resultant pellets were resuspended in 2 ml of TRIzol reagent (Life Technologies). RNA was isolated using the Zymo Direct-zol RNA miniprep kit, following the manufacturer's protocol (Zymo Research, Irvine, CA). To remove contaminating DNA, RNA samples were treated with the Turbo DNA-free kit (Life Technologies), using the rigorous DNase treatment protocol. Sequencing libraries were prepared from 3.4 μg of RNA of each sample using the ScriptSeq Complete kit (Epicentre, Madison, WI), following the protocol from the manufacturer. Samples were barcoded using the Epicentre ScriptSeq Index PCR primers 1 to 12 and combined into a single sample. Sequencing was performed at the Tufts University Core Genomics Facility using a single lane in an Illumina HiSeq 2500 sequencer run in rapid mode with single-end 100-nucleotide reads. Sequences were aligned, quantified, and tested for differential expression using Rockhopper (18).

Quantitative real-time PCR. Samples were grown as indicated for RNA-seq experiments. Three independent cultures were grown in mineral salts medium on two separate days (AKD915 average OD_{600}, 0.88 ± 0.02; AKD916 average OD_{600}, 0.72 ± 0.01). One-milliliter samples were harvested 6 h after treatment with the nitric oxide generator DPTA-NONOate and treated with RNA Protect Bacteria Reagent (Qiagen) following the manufacturer's protocol, and the resultant pellets were resuspended in 2 ml of TRIzol reagent (Life Technologies). RNA was isolated using the Zymo Direct-zol RNA miniprep kit, following the manufacturer's protocol (Zymo Research, Irvine, CA). To remove contaminating DNA, RNA samples were treated with the Turbo DNA-free kit (Life Technologies), using the rigorous DNase treatment protocol. cDNA was prepared using the Applied Biosystems high-capacity cDNA RT kit using 2 μg RNA as a template following the manufacturer's protocol. Quantitative PCR was performed using an Applied Biosystems Step One Plus PCR machine in combination with GoTaq qPCR master mix (Promega). Cycling conditions were 95°C for 1 min followed by 40 cycles of 95°C for 15 s, 55°C for 1 min, and 72°C for 1 min. The relative standard curve method was used to calculate relative expression levels using *ftsK* as an endogenous control. Data presented are averages from three separate PCR runs, one for each independent replicate. Primers are listed in Table 4.

Fluorescence-based assays for reactive oxygen species and membrane integrity. Three replicate cultures of each strain were grown in glucose mineral salts medium as described for flask-based growth. Strain AKD916 containing pAKD601Baox was grown in medium both with and without 0.1 mM IPTG. Six hours after addition of DPTA-NONOate, 0.5-ml samples were collected for analysis (AKD915 average OD_{600}, 0.72 ± 0.01; AKD916 average OD_{600}, 0.61 ± 0.01). For assays for reactive oxygen species, 1 μl of aminophenyl fluorescein (APF) (Invitrogen) was added to each sample with incubation in the dark at 28°C for 20 min. Samples were pelleted and washed twice with filter-sterilized artificial seawater (35 ppt; Instant Ocean, Blacksburg, VA). Two hundred microliters was loaded into a 96-well white microtiter plate (Corning, Corning, NY), and fluorescence was measured in a Bio-Tek Synergy H1 microplate multimode reader with excitation at 485 nm and emission at 515 nm, with gain set at 100. Data are reported as fluorescence units. The LIVE/DEAD BacLight bacterial viability kit (Invitrogen) was used for assays for membrane integrity. Components A and B were mixed in a 1:1 ratio, and 1.5 μl of the mixture was added to 0.5 ml of cell culture. Samples were incubated at room temperature for 20 min, and 200 μl was loaded per well of a 96-well white microtiter plate (Corning). Fluorescence was measured using a Bio-Tek Synergy H1 microplate multimode reader with excitation at 485 nm and emission at 530 and 630 nm, with gain set at 100. Data are reported as a ratio of green fluorescence (intact membrane) divided by red fluorescence (disrupted membrane). Each experiment was repeated three times, with results from one representative experiment shown. Significance was measured using Student's *t* test.

NAD^+/NADH assays. One-milliliter samples were collected during the flask-based growth curve assays in mineral salts medium at 6 h after addition of DPTA-NONOate to analyze NAD^+ and NADH levels (AKD915 average OD_{600}, 0.80 ± 0.01; AKD916 average OD_{600}, 0.69 ± 0.02). Samples were processed and assays performed as previously described using an enzyme cycling-based colorimetric assay (30). Absorbance data were collected using a Bio-Tek Synergy H1 Microplate Multi-Mode reader. Each experiment included three independent replicates for each strain and was performed on three separate days. Data are presented as combined averaged results from the three experiments (with error bars indicating standard error), and significance was measured using Student's *t* test.

Accession number(s). Raw Illumina reads have been deposited in the Sequence Read Archives (SRA) under SRA accession numbers SRS2800744 and SRS2800745.

SUPPLEMENTAL MATERIAL

Supplemental material for this article may be found at https://doi.org/10.1128/JB.00797-17.

SUPPLEMENTAL FILE 1, XLSX file, 0.3 MB.

ACKNOWLEDGMENTS

This work was supported by funding from the National Science foundation awarded to A.K.D. (grant MCB-1050687).

Any opinions, findings, and conclusions or recommendations expressed in this material are those of the author and do not necessarily reflect the views of the National Science Foundation.

REFERENCES

1. McDonald AE, Vanlerberghe GC. 2006. Origins, evolutionary history, and taxonomic distribution of alternative oxidase and plastoquinol terminal oxidase. Comp Biochem Physiol D Genomics Proteomics 1:357–364. https://doi.org/10.1016/j.cbd.2006.08.001.
2. Vanlerberghe GC, McIntosh L. 1997. Alternative oxidase: from gene to function. Annu Rev Plant Physiol Plant Mol Biol 48:703–734. https://doi.org/10.1146/annurev.arplant.48.1.703.
3. Meeuse BJD. 1975. Thermogenic respiration in aroids. Annu Rev Plant Physiol 26:117–126. https://doi.org/10.1146/annurev.pp.26.060175.001001.
4. Vanlerberghe G. 2013. Alternative oxidase: a mitochondrial respiratory pathway to maintain metabolic and signaling homeostasis during abiotic and biotic stress in plants. Int J Mol Sci 14:6805–6847. https://doi.org/10.3390/ijms14046805.
5. Del-Saz NF, Ribas-Carbo M, McDonald AE, Lambers H, Fernie AR, Florez-Sarasa I. 2018. An *in vivo* perspective of the role(s) of the alternative oxidase

pathway. Trends Plant Sci 23:206–219. https://doi.org/10.1016/j.tplants.2017.11.006.
6. McDonald AE, Amirsadeghi S, Vanlerberghe GC. 2003. Prokaryotic orthologues of mitochondrial alternative oxidase and plastid terminal oxidase. Plant Mol Biol 53:865–876. https://doi.org/10.1023/B:PLAN.0000023669.79465.d2.
7. McDonald AE, Vanlerberghe GC. 2005. Alternative oxidase and plastoquinol terminal oxidase in marine prokaryotes of the Sargasso Sea. Gene 349:15–24. https://doi.org/10.1016/j.gene.2004.12.049.
8. Stenmark P, Nordlund P. 2003. A prokaryotic alternative oxidase present in the bacterium *Novosphingobium aromaticivorans*. FEBS Lett 552:189–192. https://doi.org/10.1016/S0014-5793(03)00920-7.
9. Rusch DB, Halpern AL, Sutton G, Heidelberg KB, Williamson S, Yooseph S, Wu D, Eisen JA, Hoffman JM, Remington K, Beeson K, Tran B, Smith H, Baden-Tillson H, Stewart C, Thorpe J, Freeman J, Andrews-Pfannkoch C, Venter JE, Li K, Kravitz S, Heidelberg JF, Utterback T, Rogers YH, Falcon LI, Souza V, Bonilla-Rosso G, Eguiarte LE, Karl DM, Sathyendranath S, Platt T, Bermingham E, Gallardo V, Tamayo-Castillo G, Ferrari MR, Strausberg RL, Nealson K, Friedman R, Frazier M, Venter JC. 2007. The Sorcerer II Global Ocean Sampling expedition: northwest Atlantic through eastern tropical Pacific. PLoS Biol 5:e77. https://doi.org/10.1371/journal.pbio.0050077.
10. Morris RM, Rappe MS, Connon SA, Vergin KL, Siebold WA, Carlson CA, Giovannoni SJ. 2002. SAR11 clade dominates ocean surface bacterioplankton communities. Nature 420:806–810. https://doi.org/10.1038/nature01240.
11. May B, Young L, Moore AL. 2017. Structural insights into the alternative oxidases: are all oxidases made equal? Biochem Soc Trans 45:731–740. https://doi.org/10.1042/BST20160178.
12. Dunn AK, Karr EA, Wang Y, Batton AR, Ruby EG, Stabb EV. 2010. The alternative oxidase (AOX) gene in *Vibrio fischeri* is controlled by NsrR and upregulated in response to nitric oxide. Mol Microbiol 77:44–55. https://doi.org/10.1111/j.1365-2958.2010.07194.x.
13. Boettcher KJ, Ruby EG. 1990. Depressed light emission by symbiotic *Vibrio fischeri* of the sepiolid squid *Euprymna scolopes*. J Bacteriol 172:3701–3706. https://doi.org/10.1128/jb.172.7.3701-3706.1990.
14. Visick KL, Ruby EG. 2006. *Vibrio fischeri* and its host: it takes two to tango. Curr Opin Microbiol 9:632–638. https://doi.org/10.1016/j.mib.2006.10.001.
15. Davidson SK, Koropatnick TA, Kossmehl R, Sycuro L, McFall-Ngai MJ. 2004. NO means 'yes' in the squid-vibrio symbiosis: nitric oxide (NO) during the initial stages of a beneficial association. Cell Microbiol 6:1139–1151. https://doi.org/10.1111/j.1462-5822.2004.00429.x.
16. Wang Y, Dunn AK, Wilneff J, McFall-Ngai MJ, Spiro S, Ruby EG. 2010. *Vibrio fischeri* flavohaemoglobin protects against nitric oxide during initiation of the squid-*Vibrio* symbiosis. Mol Microbiol 78:903–915. https://doi.org/10.1111/j.1365-2958.2010.07376.x.
17. Cuny C, Lesbats M, Dukan S. 2007. Induction of a global stress response during the first step of *Escherichia coli* plate growth. Appl Environ Microbiol 73:885–889. https://doi.org/10.1128/AEM.01874-06.
18. McClure R, Balasubramanian D, Sun Y, Bobrovskyy M, Sumby P, Genco CA, Vanderpool CK, Tjaden B. 2013. Computational analysis of bacterial RNA-Seq data. Nucleic Acids Res 41:e140. https://doi.org/10.1093/nar/gkt444.
19. Woodmansee AN, Imlay JA. 2002. Reduced flavins promote oxidative DNA damage in non-respiring *Escherichia coli* by delivering electrons to intracellular free iron. J Biol Chem 277:34055–34066. https://doi.org/10.1074/jbc.M203977200.
20. Ruby EG, Urbanowski M, Campbell J, Dunn A, Faini M, Gunsalus R, Lostroh P, Lupp C, McCann J, Millikan D, Schaefer A, Stabb E, Stevens A, Visick K, Whistler C, Greenberg EP. 2005. Complete genome sequence of *Vibrio fischeri*: a symbiotic bacterium with pathogenic congeners. Proc Natl Acad Sci U S A 102:3004–3009. https://doi.org/10.1073/pnas.0409900102.
21. Engl C, Jovanovic G, Lloyd LJ, Murray H, Spitaler M, Ying L, Errington J, Buck M. 2009. *In vivo* localizations of membrane stress controllers PspA and PspG in *Escherichia coli*. Mol Microbiol 73:382–396. https://doi.org/10.1111/j.1365-2958.2009.06776.x.
22. Choi PS, Naal Z, Moore C, Casado-Rivera E, Abruna HD, Helmann JD, Shapleigh JP. 2006. Assessing the impact of denitrifier-produced nitric oxide on other bacteria. Appl Environ Microbiol 72:2200–2205. https://doi.org/10.1128/AEM.72.3.2200-2205.2006.
23. Millenaar FF, Lambers H. 2003. The alternative oxidase: *in vivo* regulation and function. Plant Biol 5:2–15. https://doi.org/10.1055/s-2003-37974.
24. Vanlerberghe GC, Cvetkovska M, Wang J. 2009. Is the maintenance of homeostatic mitochondrial signaling during stress a physiological role for alternative oxidase? Physiol Plant 137:392–406. https://doi.org/10.1111/j.1399-3054.2009.01254.x.
25. Miller JH. 1992. A short course in bacterial genetics, p 456. Cold Spring Harbor Laboratory Press, Cold Spring Harbor, NY.
26. Stabb EV, Reich KA, Ruby EG. 2001. *Vibrio fischeri* genes *hvnA* and *hvnB* encode secreted NAD(+)-glycohydrolases. J Bacteriol 183:309–317. https://doi.org/10.1128/JB.183.1.309-317.2001.
27. Stabb EV, Ruby EG. 2002. RP4-based plasmids for conjugation between *Escherichia coli* and members of the *Vibrionaceae*. Methods Enzymol 358:413–426. https://doi.org/10.1016/S0076-6879(02)58106-4.
28. Bose JL, Rosenberg CS, Stabb EV. 2008. Effects of *luxCDABEG* induction in *Vibrio fischeri*: enhancement of symbiotic colonization and conditional attenuation of growth in culture. Arch Microbiol 190:169–183. https://doi.org/10.1007/s00203-008-0387-1.
29. Gaudy AF, Jr, Abu-Niaaj F, Gaudy ET. 1963. Statistical study of the spot-plate technique for viable-cell counts. Appl Microbiol 11:305–309.
30. Kern SE, Price-Whelan A, Newman D. 2014. Extraction and measurement of NAD(P)+ and NAD(P)H. Methods Mol Biol 1149:311–323. https://doi.org/10.1007/978-1-4939-0473-0_26.
31. Hanahan D. 1983. Studies on transformation of *Escherichia coli* with plasmids. J Mol Biol 166:557–580. https://doi.org/10.1016/S0022-2836(83)80284-8.
32. Dunn AK, Martin MO, Stabb EV. 2005. Characterization of pES213, a small mobilizable plasmid from *Vibrio fischeri*. Plasmid 54:114–134. https://doi.org/10.1016/j.plasmid.2005.01.003.